



**HAL**  
open science

## Projection under pairwise distance controls

Hiba Alawieh, Nicolas Wicker, Christophe Biernacki

► **To cite this version:**

Hiba Alawieh, Nicolas Wicker, Christophe Biernacki. Projection under pairwise distance controls. 2019. hal-01420662v4

**HAL Id: hal-01420662**

**<https://hal.science/hal-01420662v4>**

Preprint submitted on 11 Dec 2019 (v4), last revised 23 Dec 2020 (v5)

**HAL** is a multi-disciplinary open access archive for the deposit and dissemination of scientific research documents, whether they are published or not. The documents may come from teaching and research institutions in France or abroad, or from public or private research centers.

L'archive ouverte pluridisciplinaire **HAL**, est destinée au dépôt et à la diffusion de documents scientifiques de niveau recherche, publiés ou non, émanant des établissements d'enseignement et de recherche français ou étrangers, des laboratoires publics ou privés.

1

## 2 **Projection under pairwise distance control**

3 Hiba Alawieh <sup>a</sup>, Nicolas Wicker <sup>a</sup> and Christophe Biernacki <sup>a</sup>

4 <sup>a</sup>Université Lille 1, - UFR de Mathématiques, cité scientifique, 59655 Villeneuve d'Ascq,  
5 France

### 6 **ARTICLE HISTORY**

7 Compiled December 11, 2019

### 8 **ABSTRACT**

9 Visualization of high dimensional and possibly complex data onto a low-dimensional  
10 space is often difficult. Several projection methods have been already proposed to  
11 display such high-dimensional structures on a lower-dimensional space, but the infor-  
12 mation lost is not always considered. Here, a new projection paradigm is presented to  
13 describe a non-linear projection method that takes into account the projection qual-  
14 ity of each projected point in the reduced space, this quality being directly available  
15 at the scale of this reduced space. More specifically, this novel method allows for a  
16 straightforward visualization data in  $\mathbb{R}^2$  with a simple reading of the approximation  
17 quality and thus provides a novel variant of dimensionality reduction.

### 18 **KEYWORDS**

19 Data visualization; dimensionality reduction; multidimensional scaling; principal  
20 component analysis; kernel principal component analysis.

## 21 **1. Introduction**

22 Several domains in science use data with large numbers of variables in their studies  
23 such as in biology (Cheung (2012), Golub *et al.* (1999)), chemistry (Svante *et al.*  
24 (1984)), geography (Van der Hilst *et al.* (2007)) and finance (Jagannathan and Ma  
25 (2003)). These data can be viewed as a large matrix and extracting results from this

26 type of matrix is often difficult and complicated. In such cases, it is desirable to reduce  
27 the number of dimensions of data by conserving as much information as possible from  
28 the given initial matrix.

29 Different types of multivariate data analysis methods have been developed to study  
30 these data such as dimensionality reduction, variables selection, cluster analysis and  
31 other methods. Typically, dimensionality reduction is used to summarize the data  
32 with variable selection used to choose the pertinent variables from the set of candidate  
33 variables and cluster analysis used to group the objects or variables. In our study, we  
34 focus on dimensionality reduction. Dimensionality reduction techniques can be used in  
35 different ways, to solely lower the dimensionality to prepare data for other treatments  
36 or for data visualization to provide a simple interpretation of the data in  $\mathbb{R}^2$  or  $\mathbb{R}^3$ .

37 Due to the difficulties faced by high dimensional data, many methods for data  
38 dimensionality reduction and data visualization have been proposed (Chan (2006);  
39 Chinchilli and Sen (1987); Dempster (1971); Keim and Kriegel (1996); Mardia *et*  
40 *al.* (1979)). Some of the most common methods include principal component analysis  
41 (PCA) (Jackson (1991)), multidimensional scaling (MDS) (Togerson (1958)), scatter  
42 plot matrix (Cleveland and McGill (1988)), parallel coordinates (Inselberg (1985))  
43 and Sammon's mapping (Sammon (1969)). Scatter plot matrix and parallel coordi-  
44 nates methods are widely used to visualize multidimensional data sets. An issue with  
45 principal component analysis and multidimensional scaling is that as the number of  
46 dimensions grow, important multi-dimensional relationships might not be visualized.  
47 Moreover, the quality of projection assessed by the percentage of variance that is con-  
48 served or by the stress factor is a global projection quality measure and only takes  
49 into account what happens globally. Typically, it could be a good projection globally,  
50 if the percentage of variance obtained using PCA, for example, is large.

51 In some projection methods such as PCA, a local measure is defined to indicate  
52 the projection quality of each projected point taken individually. This local measure is  
53 evaluated by the squared cosine of the angle between the principal space and the vector  
54 of the point. A good representation in the projected space is hinted by high squared  
55 cosine values. This measure is useful in cases of linear projection, which happens  
56 in PCA, but cannot be applied in the case of nonlinear projection. Moreover, linear

57 dimensionality reduction misses important nonlinear structures in the data which does  
58 not allow to give powerful results in case of nonlinear configurations. Therefore, many  
59 methods have been developed to perform nonlinear projections by nonlinearizing a  
60 linear dimensionality reduction or by using manifold learning methods.

61 The nonlinearization of linear dimensionality reduction is applied to extract nonlinear  
62 principal components. Kernel PCA is one of the most exciting methods in this domain,  
63 which integrates a kernel function to determine principal components in different high-  
64 dimensional space (Schölkopf (1998)). Manifold learning methods are an approach to  
65 construct a matrix using the neighborhood information and take a spectral decom-  
66 position to find a nonlinear embedding (like Locally Linear Embedding LLE, Isomap  
67 algorithm etc). (Lee and Verleysen (2007), Tenenbaum *et al.* (2000), Roweis and Saul  
68 (2000)).

69 In this paper, we propose a new nonlinear projection method that projects the  
70 points in a reduced space by using the pairwise distance between pairs of points and  
71 by taking into account the projection quality of each point taken individually. Nonlin-  
72 ear projection methods cited in the previous paragraph project the points in a feature  
73 space which makes the interpretation of distances between the projected points mean-  
74 ingless. In our method, the distances between projected points are related to the initial  
75 distances between points, offering a way to easily interpret the distances observed in  
76 the projection plane. This projection leads to a representation of the points as circles  
77 with a different radius associated to each point. Henceforth, this method will be re-  
78 ferred to as "Projection under pairwise distance control". Furthermore, visualization  
79 of data in a reduced space is not the only objective of this method. It can serve as a  
80 dimensionality reduction method to reduce the number of variables by minimizing the  
81 sum of the radii and to then determine the number of variables that can be kept.

82 The main contribution of this study is to provide a simple data visualization in  $\mathbb{R}^2$   
83 with a straightforward interpretation and to provide a new variant of dimensionality  
84 reduction. Firstly, the new projection method is presented in Section 2. In Section 3,  
85 the algorithms used in solving the optimization problems related to this method are  
86 then illustrated. In Section 4 the application of this method to various real data sets  
87 is shown. Finally, the conclusions are drawn in Section 5.

88 **2. Projection under pairwise distance control**

89 Let us consider  $n$  points given by their pairwise distances denoted by  $d_{ij}$  for  $i, j \in$   
90  $\{1, \dots, n\}$ . The objective is to project these points using distances into a reduced  
91 space  $\mathbb{R}^q$  by introducing additional variables, called hereafter radii, that indicate the  
92 extent to which the projection of each point is accurate. The local quality is then given  
93 by the values of the radii. A good projection quality of point  $i$  is indicated by a small  
94 radius value denoted by  $r_i$ . It is important to note that both units of  $d_{ij}$ 's and  $r_i$ 's are  
95 identical, thus allowing for a direct comparison.

96 Before presenting our method, an overview of principal component analysis, Kernel  
97 PCA and multidimensional scaling is given to highlight the significance of our method.

98 **2.1. Overview of certain existing methods: PCA, KPCA and MDS**

99 ***Principal Component Analysis (PCA)***

100 The PCA method is the most used method for data visualization and dimensional-  
101 ity reduction. This method is a linear projection technique applied when the data  
102 is linearly separable. PCA can be stated as an optimization problem involving the  
103 squared Euclidean distances (Mardia *et al.* (1979)). This optimization problem is the  
104 following:

$$\mathcal{P}_{\text{PCA}} : \begin{cases} \min_{A \in \mathcal{M}_{p \times q}} \sum_{1 \leq i < j \leq n} |d_{ij}^2 - \|Ay_i - Ay_j\|^2| \\ \text{s.t. } \text{rank}(A) = m \\ AA^T = I_p, \end{cases}$$

105 where  $y_i \in \mathbb{R}^p$  is the original coordinates vector of point  $i$ ,  $d_{ij}^2$  is the squared distance  
106 for couple  $(i, j)$  given by  $\|y_i - y_j\|^2$  and  $A$  is the projection matrix of dimension  $p \times q$   
107 with  $q$  being the reduced space dimension. By its nature, PCA cannot take into account  
108 nonlinear structures, as it describes the data in terms of a linear subspace. To deal  
109 with nonlinearity, Kernel PCA, the reproducing kernel Hilbert space variant of PCA,  
110 can be used.

111 **Kernel PCA (KPCA)**

112 The idea behind KPCA is to perform PCA in a feature space denoted by  $\mathcal{F}$ , obtained  
 113 by a nonlinear mapping of data from its original space into the feature space  $\mathcal{F}$ , where  
 114 the low-dimensional latent structure is hopefully easier to discover (Schölkopf (1998)).  
 115 The mapping function noted  $\Phi$  is considered as:

$$\begin{aligned} \Phi : \mathbb{R}^p &\rightarrow \mathcal{F} \\ Y &\rightarrow \Phi(Y) . \end{aligned}$$

117 The original data  $y_i$  is represented in the feature space as a function  $\Phi(y_i) = k(y_i, \cdot)$ ,  
 118 where  $k(\cdot, \cdot)$  is a positive kernel. Similar to PCA, KPCA is based on finding the first  
 119  $q$  eigenvectors corresponding to the  $q$  largest eigenvalues  $\lambda_i$  of the Gram matrix  $K =$   
 120  $(k_{ij})_{ij \in 1, \dots, n}$  where  $k_{ij} = k(y_i, y_j) = \langle \Phi(y_i), \Phi(y_j) \rangle$  is a chosen positive kernel. Letting  
 121  $V_v$ , for  $v = 1, \dots, q$ , are the eigenvectors in the feature space and  $P_{\Phi(y)}$  is the projection  
 122 of  $\Phi(y)$  onto the subspace  $V_1, \dots, V_q$ . The KPCA problem can be represented as a  
 123 minimization problem with the following error:

$$\mathcal{E}_{\text{KPCA}} : \|\Phi(y) - P_{\Phi(y)}\|_2^2 ,$$

124 where  $P_{\Phi(y)} = \sum_{v=1}^q \langle \Phi(y), V_v \rangle V_v$ .

125 Furthermore, the only measure used to evaluate the projection quality of points  
 126 for PCA and KPCA is the squared cosine value. Squared cosine values cannot be  
 127 interpreted at the same time as the distances in the projection because the cosine  
 128 values do not have a specific unit. More precisely, the visualization of the projection  
 129 in the reduced space using PCA and KPCA cannot simply be interpreted in terms  
 130 of original distances between the points. Indeed, in PCA, the cosine values do not  
 131 provide a quantitative assessment of the error made when considering the distances  
 132 between the projected points, all the more in KPCA where the projected points are  
 133 in the feature space so the term "distances" is not related to the distances between  
 134 the points in the original space.

135 **Multidimensional Scaling (MDS)**

136 As with PCA, Multidimensional scaling (MDS) consists of finding a new data configu-  
 137 ration in a reduced space. The main difference between these two methods is that the  
 138 input data in MDS is in the form of a similarity or dissimilarity matrix, called "prox-  
 139 imity", representing the proximity between pairs of objects. The key idea of MDS is to  
 140 perform dimensionality reduction in a way to approximate high-dimensional distances  
 141 denoted by  $\delta_{ij}$  the low-dimensional distances  $d_{ij}$ , where  $d_{ij}$  is equal to the distance  
 142 between  $x_i$  and  $x_j$ , the coordinates of  $i$  and  $j$  in the reduced space. In the classic and  
 143 simplest case of MDS, the least-squares loss function denoted by "Stress" is given as  
 144 follows:

$$\text{Stress} = \sqrt{\sum_{1 \leq i < j \leq n} (d_{ij} - \|x_i - x_j\|)^2}.$$

145 By minimizing the Stress function, we find the best configuration of  $(x_1, \dots, x_n) \in \mathbb{R}^q$   
 146 such that the distances fit to the initial distances.

147 If we consider  $n$  variables as  $r_1, \dots, r_n \in \mathbb{R}^+$ , the sum of which bounds the stress  
 148 function, the optimization problem  $\mathcal{P}_{\text{MDS}}$  can be equivalently rewritten as:

$$\mathcal{P}_{\text{MDS}} : \begin{cases} \min_{r_1, \dots, r_n \in \mathbb{R}^+} \sum_{i=1}^n r_i \\ \text{s.t.} \quad \sum_{i=1}^n r_i \geq \frac{1}{n-1} \sqrt{\sum_{1 \leq i < j \leq n} (d_{ij} - \|x_i - x_j\|)^2}. \end{cases}$$

149 A criterion to determine the local projection quality has been proposed by Born  
 150 and Groenen in Borg and Groenen (2005) called Stress-per-point (*SPP*). The *SPP*  
 151 of point  $i$  is given by:

$$SPP_i = \frac{\sum_{j=1, j \neq i}^n (d_{ij} - \|x_i - x_j\|)^2}{\frac{\sum_{j=1, j \neq i}^n d_{ij}^2}{\text{Stress}}},$$

152 with  $Stress = \frac{\sum_{1 \leq i < j \leq n}^n (d_{ij} - \|x_i - x_j\|)^2}{\sum_{1 \leq i < j \leq n}^n d_{ij}^2}$ .

153 Again, this is difficult to interpret directly on the projection as a distance error because  
 154 the projected points are not in the same metric of initial data.

155 However, we can observe that the constraint on  $\sum_{i=1}^n r_i$  can be modified to have a  
 156 stronger control on each  $d_{ij}$  in the following way:  $|d_{ij} - \|x_i - x_j\|| \leq r_i + r_j$  where  $x_i$   
 157 and  $x_j$  are the projected coordinates of points  $i$  and  $j$ .

158 Therefore, our objective is to propose a new nonlinear projection method that indi-  
 159 vidually controls the projection of points and provides a graphical representation in  
 160 the same metric as the original space with an error associated to each point.

161 **2.2. Our proposal: Projection under pairwise distance control method**

162 Letting  $x_1, \dots, x_n$  be the coordinates of the projected points in  $\mathbb{R}^p$  and  $\|x_i - x_j\|$  is  
 163 the distance between two projected points  $(i, j)$ . Radii are introduced in this paper to  
 164 assess how far  $\|x_i - x_j\|$  is from the given distance  $d_{ij}$ . Indeed, for the couple  $(i, j)$ , we  
 165 are aiming for a  $\|x_i - x_j\|$  value close to  $d_{ij}$ , which should imply a small radii  $(r_i, r_j)$ .  
 166 Figure 1 depicts this idea: for each point  $i \in \{1, \dots, n\}$ , the projection of  $i$  belongs to  
 167 a sphere with center  $x_i$  and radius  $r_i$  such that for each couple  $(i, j) \in \{1, \dots, n\}$  we  
 168 have  $\|x_i - x_j\| - (r_i + r_j) \leq d_{ij} \leq \|x_i - x_j\| + r_i + r_j$ .

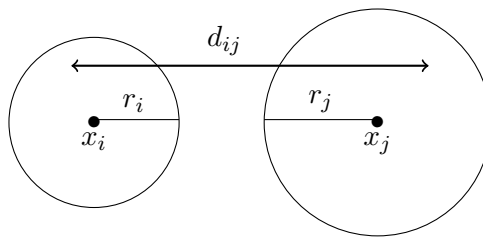


Figure 1.: Example of radii for bounding of the original distance  $d_{ij}$

169 **Radii for uncertainty metric:** The idea presented above can be expressed by  
 170 finding the value of radii that satisfy these two constraints:



- 171 •  $\sum_{i=1}^n r_i$  is minimal.
- 172 •  $d_{ij} \in [|\|x_i - x_j\| - r_i - r_j|; \|x_i - x_j\| + r_i + r_j]$ , for  $1 \leq i < j \leq n$ .

173 The projection under pairwise distance control problem can be written as the following  
 174 optimization problem:

$$\mathcal{P}_{r,x} : \begin{cases} \min_{r_1, \dots, r_n \in \mathbb{R}^+, x_1, \dots, x_n \in \mathbb{R}^q} \sum_{i=1}^n r_i \\ \text{s.t. } |d_{ij} - \|x_i - x_j\|| \leq r_i + r_j, \text{ for } 1 \leq i < j \leq n \end{cases}$$

175 **Linear optimization program using fixed coordinates  $(x_1, x_2, \dots, x_n)$ :** Of  
 176 course, by fixing the coordinates vectors  $x_i$  for all  $i \in \{1, \dots, n\}$  using principal com-  
 177 ponent analysis or any other projection method, the optimization problem can easily  
 178 be solved in  $(r_1, \dots, r_n)$  using linear programming. This problem can be written as  
 179 follows:

$$\mathcal{P}_r : \begin{cases} \min_{r_1, \dots, r_n \in \mathbb{R}^+} \sum_{i=1}^n r_i \\ \text{s.t. } |d_{ij} - \|x_i - x_j\|| \leq r_i + r_j, \text{ for } 1 \leq i < j \leq n \end{cases}$$

180 It should be noted that a solution for problem  $\mathcal{P}_r$  always exists. Indeed, to satisfy the  
 181 constraints it is sufficient to increase all  $r_i$ . Thus, for any method producing points in  
 182 a reduced space as PCA for instance, we can compute the radii as a post-processing  
 183 to assess the local quality of the projected points.

184  **$\mathcal{P}_{r,x}$  is a non-convex optimization problem:** For any dimension  $p$ , even with  
 185  $p = 1$ , note that the optimization problem  $\mathcal{P}_{r,x}$  is not convex. Indeed, to easily illustrate  
 186 this fact, we take 4 points with an arbitrary order indexed by  $i_1, i_2, i_3$  and  $i_4$  in  $\mathbb{R}$   
 187 with respective coordinates  $x_{i_1} = 0, x_{i_2} = 2, x_{i_3} = 3$  and  $x_{i_4} = 1$ . Note that distances  
 188  $d_{i_1 i_2}$  and  $d_{i_3 i_4}$  are both equal to 2.

189 Let us consider the function  $g(x_i, x_j) = |d_{ij} - \|x_i - x_j\||$ . Thus, we have  $g(x_{i_1}, x_{i_2}) = 0$   
 190 and  $g(x_{i_3}, x_{i_4}) = 0$  but  $g(\frac{x_{i_1} + x_{i_3}}{2}, \frac{x_{i_2} + x_{i_4}}{2}) = |0 - 2| = 2$  which is larger than  
 191  $\frac{g(x_{i_1}, x_{i_2}) + g(x_{i_3}, x_{i_4})}{2} = 0$  proving non convexity associated to this sample design.

In fact, problem  $P_{r,x}$  is convex in one dimension only if  $x_{i_1}, x_{i_2}, \dots, x_{i_n}$  are ordered. Indeed, let us consider  $x_{i_4} \leq x_{i_3} \leq x_{i_2} \leq x_{i_1}$  so that  $g(x_{i_1}, x_{i_2}) = |x_{i_1} - x_{i_2} - d_{i_1 i_2}|$  and  $g(x_{i_3}, x_{i_4}) = |x_{i_3} - x_{i_4} - d_{i_3 i_4}|$  so that for any  $\lambda, \mu \geq 0$ :

$$g\left(\frac{\lambda x_{i_1} + \mu x_{i_3}}{\lambda + \mu}, \frac{\lambda x_{i_2} + \mu x_{i_4}}{\lambda + \mu}\right) = \left| \frac{\lambda}{\lambda + \mu}(x_{i_1} - x_{i_2} - d_{i_1 i_2}) + \frac{\mu}{\lambda + \mu}(x_{i_3} - x_{i_4} - d_{i_3 i_4}) \right| \\ \leq \frac{\lambda}{\lambda + \mu} g(x_{i_1}, x_{i_2}) + \frac{\mu}{\lambda + \mu} g(x_{i_3}, x_{i_4}),$$

192 which proves convexity. Therefore given an ordering, we have a convex optimization  
 193 each time that can be solved exactly and the global optimum can be found by taking  
 194 the minimum obtained for all permutations of  $x_1, \dots, x_n$ . However, this only works in  
 195 one dimension at a time; an approximate non-convex optimization is needed since we  
 196 have multidimensional data.

197 Many methods available in the literature propose different ways to solve such opti-  
 198 mization problems. Examples include: trust-region-reflective (Conn *et al.* (2000)),  
 199 which chooses and computes an approximation of the objective function, and then  
 200 chooses and modifies the trust region and finally solves the trust-region subproblem;  
 201 sequential quadratic programming (SQP) which solves the optimization problem by  
 202 addressing a sequence of quadratic programming problems where the Lagrangian func-  
 203 tion is approximated by a quadratic function and the constraints are approximated by  
 204 a linear hyper-space (Boggs and Tolle (1995)); the active-set method, which is com-  
 205 posed of two phases, wherein for the first phase (the feasibility phase) the objective  
 206 function is ignored while a feasible point is found for the constraints, and in the sec-  
 207 ond phase (the optimality phase) the objective function is minimized while feasibility  
 208 is maintained (Wong (2011), Cristofari *et al.* (2007)). The choice of optimization  
 209 method to use to achieve optimality of the optimization problem is essential and de-  
 210 pends on many factors such as the type of problem, desired quality of solution, time  
 211 limit and availability of the algorithm implementation etc. In fact, all of the methods  
 212 cited above can be used in optimizing problem  $\mathcal{P}_{r,x}$  which is a constrained optimiza-  
 213 tion problem having inequalities constraints and they are all available in MATLAB  
 214 using the function "fmincon" for constrained nonlinear optimization problems (since

215 the proposed method is implemented in MATLAB). Having small radii is the main  
216 constraint in our optimization problem thus, the objective is to obtain good solution  
217 within a reasonable and practical timeframe. Therefore, a method that balances time  
218 and quality of the solution is required.

219 **Another strategy of use: Dimensionality reduction** One of the main objectives  
220 of high-dimensional data studies is to choose, from a large number of variables, those  
221 that are important for understanding the underlying studied phenomena. In addition  
222 to visualization, our aim can thus be to reduce the dimension rather than to visualize  
223 data in  $\mathbb{R}^2$ . Therefore, the proposed method can serve to reduce the number of variables  
224 by taking into account the minimal value of  $\sum_{i=1}^n r_i$ . Indeed, by solving the problem  
225  $\mathcal{P}_{r,x}$  using different dimension values, we can choose the dimension with respect to the  
226 local projection quality promoted in this study.

### 227 *2.3. A toy example for illustrating our method*

228 Let us apply the proposed projection method to a simple example by taking a tetrahe-  
229 dron with all pairwise distances equal to 1. For problem  $\mathcal{P}_r$ , the coordinates of points  
230  $x_i$  for  $i = 1, \dots, 4$  are obtained using multidimensional scaling. The optimization was  
231 carried out using the MATLAB software with the optimization toolbox for linear and  
232 nonlinear optimization problem used for problems  $\mathcal{P}_r$  and  $\mathcal{P}_{r,x}$ , respectively. The value  
233 of  $\sum_{i=1}^4 r_i$  is equal to 0.7935 for problem  $\mathcal{P}_r$  and 0.4226 for  $\mathcal{P}_{r,x}$ . It is clear that prob-  
234 lem  $\mathcal{P}_{r,x}$  gives better solutions than problem  $\mathcal{P}_r$  with smaller radii, which indicates  
235 better projection quality of points.

236 This result can be shown in Figure 2, which depicts the solution obtained using  $\mathcal{P}_r$   
237 and  $\mathcal{P}_{r,x}$ . In Figures 2a and 2b, the circles with different radii indicate the quality of  
238 projection for each point. The circle color is related to the radius value, the shades of  
239 gray lie between white and black in the descending direction of the radius values; the  
240 smaller the radius, the darker circle. The points that have circles with small radii are  
241 also considered as projected points. Note that the points represented as points and  
242 not as circles are very well projected, having radii almost equal to zero.

243 In Figure 2b, just one circle appears indicating that the projection quality using prob-

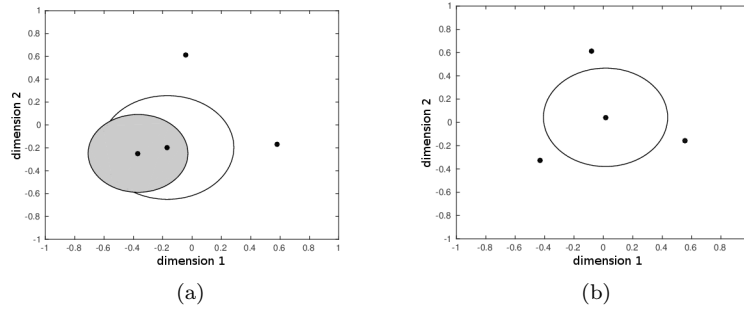


Figure 2.: Projected points after solving problem  $\mathcal{P}_r$  and problem  $\mathcal{P}_{r,x}$ . The x-axis and y-axis are dimension 1 and dimension 2, respectively. (a) and (b) show the projection obtained from the solution of problem  $\mathcal{P}_r$  using MDS and of problem  $\mathcal{P}_{r,x}$  respectively.

244 lem  $\mathcal{P}_{r,x}$  is better than when using problem  $\mathcal{P}_r$ . In Figure 2a, half of the points are  
 245 well projected whereas the other half have large radii, indicating that they are not well  
 246 projected. Moreover, it is worth noting that the three outer points all have radii equal  
 247 to 0, which indicates that they are all perfectly placed with respect to one another.

248 In Figure 2b, the distances between the three points that are very well projected  
 249 are equal to the distances between these points in their original space ( $d_{kl} = \|x_k -$   
 250  $x_l\|$  where  $k$  and  $l$  are two very well projected points) whereas the distances from  
 251 the badly projected points to the perfectly projected points are not yet conserved.  
 252 Therefore, using the proposed method, we have succeeded in conserving half of the  
 253 original distances in the new projection plane and the other half have been changed  
 254 to fit the new configuration. If we now apply the proposed method to the distances  
 255 obtained by MDS to find the radius of each projected point (Figure 2a), it can be noted  
 256 that one distance is conserved as the original distance and the other five distances  
 257 are changed which indicates that the proposed method projects the points well by  
 258 conserving the distances between the points as much as possible.

259 It is also important to note that, in general, our method is not only a nonlinear  
 260 projection method with local quality measure, but it can act as a new tool to give  
 261 the local quality of projection for the classical projection methods using the radii by  
 262 solving problem  $\mathcal{P}_r$ . It can be used outside our method as post-processing of classical  
 263 methods.

264 **2.4. Connexion with existing methods**

265 Multidimensional fitting (MDF) (Berge *et al.* (2010)) is a method that modifies the  
 266 coordinates of a set of points in order to make the distances calculated on the modified  
 267 coordinates similar to a given set of distances on the same set of points. The so-called  
 268 "target matrix", the matrix that contains the point coordinates and "reference matrix"  
 269 is the matrix that contains the given distances.

270 Let us take  $X = \{x_1 | \dots | x_n\}$ , the target matrix of coordinates and  $D = \{d_{ij}\}$ , the  
 271 reference matrix of distances. The objective function of MDF problem is given by:

$$\sum_{1 \leq i < j \leq n} |d_{ij} - \|x_i - x_j\||.$$

272 **Proposition 2.1.** *Problem  $\mathcal{P}_{r,x}$  is bounded from below by  $\frac{1}{n-1} \sum_{1 \leq i < j \leq n} |d_{ij} - \|x_i - x_j\||$*   
 273 *where  $x_1, \dots, x_n$  is the optimum for the associated MDF problem.*

274 **Proof.** By summing all the constraints of problem  $\mathcal{P}_{r,x}$ , we obtain:

$$\sum_{1 \leq i < j \leq n} |d_{ij} - \|x_i - x_j\|| \leq \sum_{1 \leq i < j \leq n} (r_i + r_j) = (n-1) \sum_{i=1}^n r_i.$$

275 So,  $\sum_{i=1}^n r_i \geq \frac{1}{n-1} \sum_{1 \leq i < j \leq n} |d_{ij} - \|x_i - x_j\||$ , which concludes the proof.  $\square$

276 **3. Optimization tools for performing the proposed method**

277 Problem  $\mathcal{P}_{r,x}$  can be solved using different initialization points for the coordinate  
 278 matrix  $X$ . In this section, we first discuss the different initialization points of the  
 279 proposed optimization problem and then propose two algorithms to be used in our  
 280 optimization.

281 **3.1. Initialization point for problem  $\mathcal{P}_{r,x}$**

282 Different solutions of problem  $\mathcal{P}_{r,x}$  can be obtained using different initial values of  
 283 matrix  $X$ . We have considered three possibilities:

284 **1- Initial point using a known projection method** The first possibility is to  
 285 use the matrix obtained by PCA or another projection method. The choice of method  
 286 must be based on the type of data. In this application, we use PCA for quantitative  
 287 data and MDS for categorical and functional data.

288 **2- Initial point using squared distances** The optimization problem  $\mathcal{P}_{r,x}$  can be  
 289 changed by taking the squared distances between points instead of the distances.  
 290 Rewriting  $r_i^2$  as  $R_i$ , the problem is changed into

$$\mathcal{P}_{R,x} : \begin{cases} \min_{R_1, \dots, R_n \in \mathbb{R}^+, x_1, \dots, x_n \in \mathbb{R}^k} \sum_{i=1}^n R_i \\ \text{s.t. } |d_{ij}^2 - \|x_i - x_j\|^2| \leq R_i + R_j, \text{ for } 1 \leq i < j \leq n. \end{cases}$$

291 This transformation is interesting because if the constraints of problem  $\mathcal{P}_{R,x}$  are sat-  
 292 isfied, the constraints of problem  $\mathcal{P}_{r,x}$  will also be satisfied. Indeed,

$$|d_{ij}^2 - \|x_i - x_j\|^2| \leq R_i + R_j = r_i^2 + r_j^2.$$

If without loss of generality,  $d_{ij} \geq \|x_i - x_j\|$ , we obtain:

$$(d_{ij} - \|x_i - x_j\|)(d_{ij} + \|x_i - x_j\|) \leq r_i^2 + r_j^2 \leq (r_i + r_j)^2 \Rightarrow \\ |d_{ij} - \|x_i - x_j\||^2 \leq (r_i + r_j)^2 \Rightarrow |d_{ij} - \|x_i - x_j\|| \leq (r_i + r_j).$$

293 In this way problem  $\mathcal{P}_{R,x}$  can serve as an initial step in solving problem  $\mathcal{P}_{r,x}$ .

294 **3- Initial point using an improved solution of problem  $\mathcal{P}_r$**  This strategy is  
 295 more involved. First, we need two properties that provide a way to improve the opti-  
 296 mization results of problem  $\mathcal{P}_{r,x}$ .

**Proposition 3.1.** *Let us consider a point  $x_i$  such that for an index  $j$ , the following inequality is saturated:*

$$|d_{ij} - \|x_i - x_j\|| \leq r_i + r_j,$$

297 *and the other inequalities involving  $i$  are not saturated. The corresponding solution*  
 298 *can then be improved by moving  $x_i$  along the line  $x_j - x_i$  in order to decrease  $r_i$  and*  
 299  *$|d_{ij} - \|x_i - x_j\||$ .*

300 Another manner to improve the resolution of problem  $\mathcal{P}_{r,x}$  is to perform a scale  
 301 change by multiplying the coordinates  $x_i$ , for  $i = 1, \dots, n$ , by a constant  $a \in \mathbb{R}$ . Thus,  
 302 the new optimization problem is given by:

$$\mathcal{P}_{r,a} : \begin{cases} \min_{r_1, \dots, r_n, a \in \mathbb{R}^+} \sum_{i=1}^n r_i \\ \text{s.t. } |d_{ij} - a\|x_i - x_j\|| \leq r_i + r_j. \end{cases}$$

303 **Proposition 3.2.** *Let  $r_1, \dots, r_n; x_1, \dots, x_n$  be a feasible solution of  $\mathcal{P}_{r,x}$ , if  $\exists a$  such*  
 304 *that  $\eta(a) < \sum_{i=1}^n r_i$  with  $\eta(a) = \sum_{1 \leq i < j \leq n} |d_{ij} - a\|x_i - x_j\||$ , then  $\exists \tilde{r}_1, \dots, \tilde{r}_n$  a solution*  
 305 *of  $\mathcal{P}_{r,a}$  such that  $\sum_{i=1}^n \tilde{r}_i < \sum_{i=1}^n r_i$ .*

306 The new initial point called  $X_{imp}$ , is the improved solution given by using these two  
 307 properties as follows:

- 308 • Firstly, improving the solution of problem  $\mathcal{P}_r$  by solving problem  $\mathcal{P}_{r,a}$  and using  
 309 proposition 3.2.
- 310 • Secondly, improving the solution of problem  $\mathcal{P}_{r,a}$  using proposition 3.1.

### 311 **3.2. A deterministic strategy: Algorithm 1**

312 As discussed, three possibilities of coordinate matrix  $X$  can be used as the initial point:

- 313 1- Coordinates given by PCA or MDS:  $X_{\mathcal{P}_{PCA/MDS}}$  is the coordinate matrix obtained  
 314 by applying PCA or MDS and  $r_{\mathcal{P}_r}$  is a vector that contains the radius of each

- 315 point obtained by solving  $\mathcal{P}_r$ .
- 316 2- Coordinates given by squared distances:  $X_{\mathcal{P}_{R,x}}$  is the coordinate matrix obtained  
317 by solving problem  $\mathcal{P}_{R,x}$  and  $R_{\mathcal{P}_{R,x}} = r_{\mathcal{P}_{R,x}}^2$  is a vector that contains the squared  
318 radius for each point obtained by solving the subsequent  $\mathcal{P}_{R,x}$  problem.
- 319 3- Coordinates given by improving the solution of problem  $\mathcal{P}_r$ :  $X_{imp}$  is the coordi-  
320 nate matrix obtained by improving the previous solution using Proposition 3.1  
321 and  $r_{imp}$  is a vector that contains the radius of each point obtained after each  
322 iteration of solving problem  $\mathcal{P}_{r,a}$

323 Finding these matrices requires solving the following optimization problems:  $\mathcal{P}_r$ ,  
324  $\mathcal{P}_{R,x}$  and  $\mathcal{P}_{r,a}$ . Problems  $\mathcal{P}_r$  and  $\mathcal{P}_{r,a}$  are both constrained linear optimization problems  
325 that can be solved using interior-point or simplex algorithms, which are the most  
326 widely used algorithms for linear programming. The interior-point algorithm uses a  
327 primal-dual predictor-corrector algorithm and the simplex algorithm uses a systematic  
328 procedure for generating and testing candidate vertex solutions to a linear program  
329 (Murty (1983)). On the contrary, problem  $\mathcal{P}_{R,x}$  is a nonlinear optimization problem  
330 that can be solved using one of the nonlinear optimization algorithms cited in Section  
331 2.2. All these algorithms are available in MATLAB using the optimization toolbox  
332 and can be used for the corresponding problem.

333 To find the best solution of problem  $\mathcal{P}_{r,x}$ , we solve it with the three different initial-  
334 ization matrices described above. For this task, we define Algorithm 1 that gives the  
335 best solution using the different coordinate matrices. This algorithm consists of two  
336 steps, an initialization step and an optimization step. The initialization step offers  
337 three different coordinate matrices to be used in the optimization step as an initial  
338 point to quickly reach the best solution. During the optimization step, problem  $\mathcal{P}_{r,x}$   
339 is solved using one of the nonlinear optimization algorithms mentioned in Section 2.2,  
340 starting each time with one matrix of the three initial matrices already found.

341 Thus, for Algorithm 1, described below, the three different initialization matrices are  
342 tried and then the best one is chosen that gives the minimum value of  $\sum_{i=1}^n r_i$ .



---

**Algorithm 1**

---

Input:  $D$ : distance matrix,  $N$ : number of iterations.

**Initialization step**

Project the points using PCA or MDS.

Solve  $\mathcal{P}_r$  using a linear optimization method. Obtained solution:  $(X_{\mathcal{P}_{PCA/MDS}}, r_{\mathcal{P}_r})$ .

Solve  $\mathcal{P}_{R,x}$  using a nonlinear optimization method and starting from the solution of  $\mathcal{P}_r$  obtained at the previous step. Obtained solution:  $(X_{\mathcal{P}_{R,x}}, R_{\mathcal{P}_{R,x}})$ .

$X_{imp} \leftarrow X_{\mathcal{P}_{R,x}}$ .

**for**  $t = 1$  to  $N$  **do**

    Solve  $\mathcal{P}_{r,a}$  starting from  $X_{imp}$  using a linear optimization method.

    Improve the solution of  $\mathcal{P}_{r,a}$ . Obtained solution:  $(X_{imp}, r_{imp})$ .

**end for**

**Optimization step**

Optimize  $\mathcal{P}_{r,x}$  using a nonlinear optimization method and starting from  $X_{\mathcal{P}_{PCA/MDS}}$ ,  $X_{\mathcal{P}_{R,x}}$  and  $X_{imp}$ .

Choose the minimal solution obtained by these three different starting points.

---

343 **3.3. A stochastic strategy: Algorithm 2**

344 Problem  $\mathcal{P}_{r,x}$  is a hard problem, thus it is natural to resort to stochastic optimization  
345 methods. In the present case, we resort to the Metropolis-Hastings algorithm (Jo-  
346 hansen and Evers (2007)) which allows us to build a Markov chain with the desired  
347 stationary distribution. The challenging parts are the choice of the proposal distri-  
348 bution and the necessity to solve the problem  $\mathcal{P}_r$  at each iteration. Specifically, the  
349 Metropolis-Hastings algorithm requires:

350 1- A *target distribution*:

351 The target distribution is related to the objective function of problem  $\mathcal{P}_{r,x}$   
352 and is given by:

353 
$$\pi(x) \propto \exp\left(\frac{-E(x)}{T}\right),$$

354 where  $E$  is an application given by:

355 
$$E : \mathbb{R}^n \mapsto \mathbb{R}$$
  
356 
$$x = (x_1, \dots, x_n) \mapsto E(x) = \text{Solution of problem } \mathcal{P}_r \text{ with fixed } x.$$

357 The variable  $T$  is the temperature parameter, to be fixed according to the value  
358 range of  $E$ .

359 2- A *proposal distribution*:

360 The choice of the proposal distribution is very important to obtain mean-  
361 ingful results. It should be chosen in such a way that the proposal distribution

362 approaches the target distribution. The proposal distribution  $q(X \rightarrow \cdot)$  is con-  
 363 structed as follows, giving priority to the selection of points involved in saturated  
 364 constraints:

365 ○ For each point  $i$ , choose a point  $j^{(i)}$  with probability equal to:

$$P_{j^{(i)}} = \frac{\lambda \exp(-\lambda(r_i + r_{j^{(i)}} - |d_{ij^{(i)}} - \|x_i - x_{j^{(i)}}\||))}{\sum_{k=1, k \neq i}^n \lambda \exp(-\lambda(r_i + r_k - |d_{ik} - \|x_i - x_k\||))}$$

366 ○ Choose a constant  $c_{ij^{(i)}}$  using Gaussian distribution  $\mathcal{N}_k(0, \sigma)$ .

367 ○ Generate a matrix  $X^*$  by moving each vector  $x_i$  of matrix  $X^{t-1}$  as follows:

368

369 – If  $d_{ij^{(i)}} - \|x_i - x_{j^{(i)}}\| > 0$  then  $x_i^* = x_i + |c_{ij^{(i)}}|L_{ij^{(i)}}$ .

370 – else  $x_i^* = x_i - |c_{ij^{(i)}}|L_{ij^{(i)}}$ ,

371 where  $L_{ij^{(i)}} = \frac{x_i - x_{j^{(i)}}}{\|x_i - x_{j^{(i)}}\|}$ .

372 3- A linear optimization problem:

373 For the matrix  $X$  generated at each iteration, we solve the linear optimization  
 374 problem  $\mathcal{P}_r$ .

375 Algorithm 1 and Algorithm 2 are both implemented in MATLAB and a code for  
 376 each algorithm can be provided by the authors upon request.

## 377 4. Numerical applications

378 The projection method presented has been applied to different types of real data sets  
 379 and also to a simulated data set to illustrate its practical interest.

### 380 4.1. Experimental setup

381 In practice, we have tested the proposed method on the different simulated and real  
 382 data sets by solving the optimization problem  $\mathcal{P}_{r,x}$  using Algorithm 1 in addition  
 383 to the proposed Metropolis-Hastings algorithm (Algorithm 2). A distance matrix is  
 384 required each time. For the quantitative data, the Euclidean distance between points

385  $y_i \in \mathbb{R}^p$ , for  $i = 1, \dots, n$ , is computed by the known formula  $d_{ij} = \sqrt{\sum_{k=1}^p (y_{ik} - y_{jk})^2}$ .

386 For categorical data, the distance between two soybean diseases  $(i, j)$  is given through  
 387 Eskin dissimilarity (or proximity) measure (Boriah *et al.* (2008)) computed by the

388 formula  $p_{ij} = \sum_{t=1}^Q w_t p_{ij}^t$  where  $p_{ij}^t = \begin{cases} 1 & \text{if } i^t = j^t \\ \frac{n_t^2}{n_t^2 + 2} & \text{else} \end{cases}$ ,  $p_{ij}^t$  is the per-attribute

389 Eskin dissimilarity between two values for the categorical attribute indexed by  $t$ ,  $w_t$  is  
 390 the weight associated to the attribute  $t$  called  $w_t$  which is defined by:  $w_t = \frac{1}{Q}$ ,  $Q$  is the  
 391 number of attributes and  $n_t$  is the number of values taken by each attribute. Then,  
 392 using the following formula that transforms dissimilarities into similarities:  $s_{ij} = 1 - p_{ij}$ ,  
 393 the distances can be obtained by the standard transformation formula converting  
 394 similarities to distances:  $d_{ij} = \sqrt{s_{ii} - 2s_{ij} + s_{jj}}$ .

395 In addition, to compute the distances between the curves of functional data, we have  
 396 chosen a measure of proximity similar to that studied by Ieva *et al.* (2012). In their  
 397 paper, the authors develop a proper classification designed to distinguish the group-  
 398 ing structures by using a functional k-means clustering procedure with three sorts  
 399 of distances. For our work we chose one of these three proximity measures as their  
 400 results are similar. The proximity measure chosen between two curves  $F_i$  and  $F_j$  is  
 401 the following:  $d_0(F_i, F_j) = \sqrt{\int_{\mathcal{T}} (F_i^0(t) - F_j^0(t))^2 dt}$ . This measure is calculated using  
 402 the function `metric.lp()` of the `fda.usc` package for the **R** software (Febrero-Bande and  
 403 Oviedo de la Fuente (2011)).

404 To solve the different optimization problems presented in Algorithm 1, we used  
 405 the optimization toolbox available in MATLAB. For problems  $\mathcal{P}_r$  and  $\mathcal{P}_{r,a}$ , we first  
 406 applied PCA for quantitative data and MDS for categorical and functional data; a lin-  
 407 ear programming package was then used to solve the optimization problems with an  
 408 interior-point algorithm. Problems  $\mathcal{P}_{r,x}$  and  $\mathcal{P}_{R,x}$  are nonlinear optimization problems;  
 409 therefore, we used a nonlinear programming package to solve them. The algorithms  
 410 cited in Section 2.2 can be used here but we recommend to use the active-set algo-  
 411 rithm. Indeed, to choose the best algorithm in our optimization problems, we tried the  
 412 different algorithms and chose the algorithm that gives the smallest value of  $\sum_{i=1}^n r_i$  in  
 413 the shortest time compared to the other algorithms.

414 Algorithm 2 can provide a good solution if the parameters  $\lambda$ ,  $\sigma$  and  $T$  are chosen  
 415 adequately. For instance,  $\lambda$  should be such that the points belonging to unsaturated  
 416 constraints are chosen with small probabilities. Therefore, we took it equal to 100. For  
 417 the other parameters  $\sigma$  and  $T$ , we took their values in the range from 0.01 to 100.

418 Moreover, the visualization of the projection of each point  $i$  in  $\mathbb{R}^2$  is represented  
 419 as a circle having  $x_i$  as the center and  $r_i$  as the radius in a two-dimensional space,  
 420 where the horizontal and vertical axes correspond to the first and the second dimension  
 421 associated to the projection in  $\mathbb{R}^2$ , respectively. The projected point belongs to this  
 422 circle and this is the specificity of our method. For each data set, the circles obtained  
 423 for each point after solving the optimization problem  $\mathcal{P}_{r,x}$  are shown. To compare the  
 424 projection quality of our representation with that obtained by PCA and KPCA, we  
 425 used the squared cosine values as projection quality, and for MDS, the Stress-per-point  
 426 (*SPP*). Indeed, for PCA and KPCA, we plotted the projected points indexed by their  
 427 squared cosine values and for MDS, we used the smacof package in R to compute the  
 428 stress-per-point and to plot the bubble plot represented the stress-per-point.

#### 429 **4.2. A simulation study**

430 To evaluate the performance of projection under pairwise distance control method,  
 431 we conducted a simulation study. We generated 100 random samples of  $y_i$  from a 5-  
 432 dimensional multivariate normal distribution with mean  $\mathbf{0}$  and covariance matrix  $I$ ,  
 433 the identity matrix, and we calculated the Euclidean distances between pairs  $(y_i, y_j)$   
 434 for  $1 \leq i < j \leq n$ . The projection result was compared with those obtained by KPCA.

435  
 436 Figure 3 shows the results of the projection of the simulated data using the proposed  
 437 method and KPCA. By comparing Figure 3a and Figure 3b, it can be shown that  
 438 the projection quality of points using KPCA is somehow dependent on the position  
 439 of the points in the reduced space. Indeed, the projection is likely to give better  
 440 local projection quality if the projected point is located near to the center  $(0, 0)$ . On  
 441 the contrary, the proposed method gives local projection quality without giving any  
 442 importance to the position of the points in the reduced space. This result can also be  
 443 shown in the real data sets.

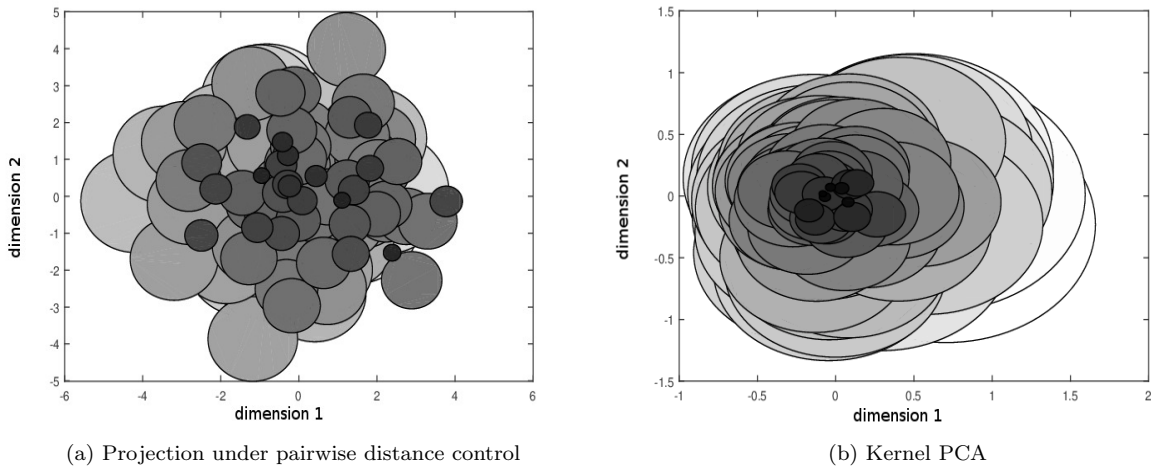


Figure 3.: Projection of the simulated data using the proposed method (a) and Kernel PCA (b).

444 This simulated data illustrates the originality and the efficiency of the proposed  
 445 method in giving a good local projection quality.

446 **4.3. Introducing the real data sets**

447 Four real data sets were used and divided into three categories:

- 448 • Quantitative data: Iris and car data sets.
- 449 • Categorical data: Soybean data set.
- 450 • Functional data: Coffee data set.

451 The Iris data set (Anderson (1935)) is a famous data set and is presented to show  
 452 that the projection works as expected. This data set contains 3 classes of 50 instances  
 453 each, where each class refers to a species of Irises. The four variables studied in this  
 454 data set are: sepal length, sepal width, petal length and petal width (in *cm*). The car  
 455 data set (Saporta (2006)) is a data set studied in the book by Saporta (Table 17.1,  
 456 page 428). This data set describes 18 cars according to various variables (cylinders,  
 457 power, length, width, weight and speed).

458 The soybean data set (Stepp (1984)) from *UCI Machine Learning Repository* char-  
 459 acterizes 47 soybean disease case histories defined over 35 attributes. Each observation  
 460 is identified by one of the 4 diseases: Diaporthe Stem Canker (D1), Charcoal Rot (D2),

461 Rhizoctonia Root Rot (D3) and Phytophthora Rot (D4).

462 The coffee data set is a time series data set used in chemometrics to classify food  
 463 types. It is a functional data set where 56 samples of coffee are available with 286  
 464 timestamps for each sample (as a result of spectroscopic analysis). This kind of time  
 465 series is common in many applications in food safety and quality assurance and was  
 466 taken from the *UCR time Series Classification and Clustering* website (Chen *et al.*  
 467 (2015)). *Coffea Arabica* and *Coffea Canephora* variant Robusta are the two species of  
 468 coffee bean that have acquired a worldwide economic importance, and many methods  
 469 have been developed to discriminate between these two species by chemical analysis  
 470 (Briandet *et al.* (1996)).

#### 471 4.4. Results from the real data sets

##### 472 4.4.1. Data visualization in $\mathbb{R}^2$

473 The optimization results for these four data sets are given in Table 1. For each data,  
 474 the sum of radii  $\sum_{i=1}^n r_i$  obtained using Algorithm 1 and Algorithm 2 is provided.

Table 1.: Solution of problem  $\mathcal{P}_{r,x}$  for data sets using Algorithm 1 and Algorithm 2.

	$\sum_{i=1}^n r_i$	
	Algorithm 1	Algorithm 2
Iris	16.19	17.2
Cars	3.27	3.35
Soybean	3.98	3.93
Coffee	21.68	21.97

475 Based on Table 1, the solutions of Algorithm 2 for the different data sets are shown  
 476 to be very close to those obtained using Algorithm 1. Thus, the radii obtained are  
 477 estimated to be close to the optimum. Moreover, it is interesting to note here that the  
 478 number of iterations  $N$  in Algorithm 1 has an important role in finding the minimal  
 479 value of  $\sum_{i=1}^n r_i$  for problem  $\mathcal{P}_{r,a}$  and then for problem  $\mathcal{P}_{r,x}$  and also to reduce the  
 480 computer speed time. In fact, the important decrease in the value of  $\sum_{i=1}^n r_i$  occurred  
 481 in the first 500 iterations through the loop of 1000 iterations, and then a small decrease

482 occurred after 500 iterations. This small decrease in value of  $\sum_{i=1}^n r_i$  after 500 iterations  
 483 shows that a size of 500 iterations can be a good choice for the Algorithm 1 since all  
 484 the studied data sets are concerned. Indeed, this result can be observed for all data  
 485 sets presented in our application with approximately 500 iterations.

486 **Iris data set:** Figure 4 depicts the result of projection under pairwise distance control  
 487 for the Iris data set. In the projection of the Iris data set shown in Figure 4, it is  
 488 interesting to note that the two areas are well separated. This corresponds to the well-  
 489 known fact that Iris versicolor and virginica are close whereas the species Iris setosa  
 490 are more distant.

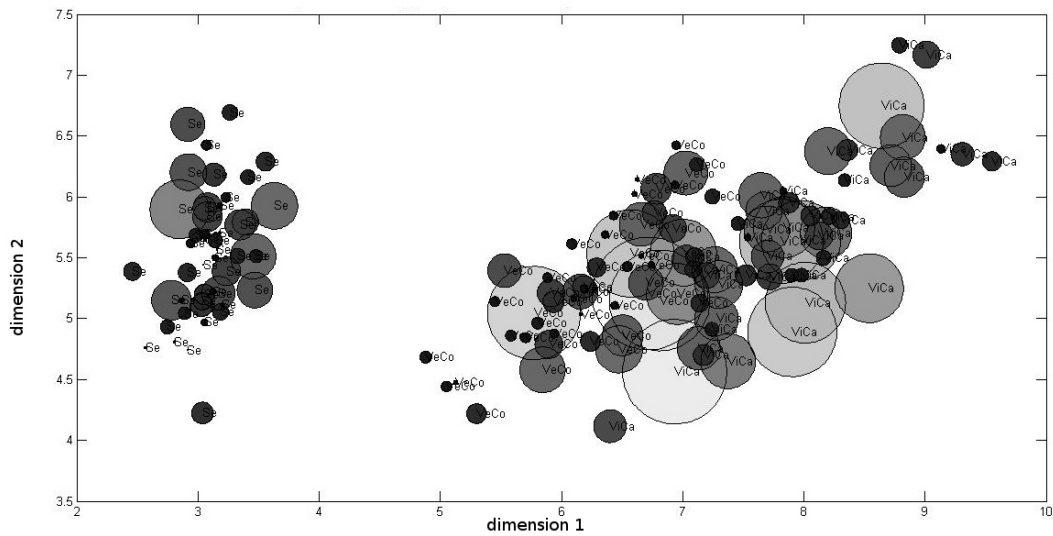


Figure 4.: Projection of the Iris data set using projection under pairwise distance control method. Two well separated groups can be observed.

491 Referring to the original data, the Iris data set contains three classes corresponding  
 492 to the three types of Iris plants and one class is linearly separable from the other two  
 493 classes. This result clearly appears in our projection.

494 Moreover, we have compared the local projection quality of PCA, KPCA and MDS  
 495 with the local projection quality obtained using projection under pairwise distance  
 496 control. By comparing the projection of PCA with the projection of our method for  
 497 the Iris data set given respectively in Figures 5 and 4, we can say that our method  
 498 projected the points without giving any importance to any group. Indeed, Figure 5  
 499 depicts a group with small values of quality measure and another group with high

500 values of quality measure, whereas the radii obtained by projection under pairwise  
 501 distance control method are distributed in an equivalent way.

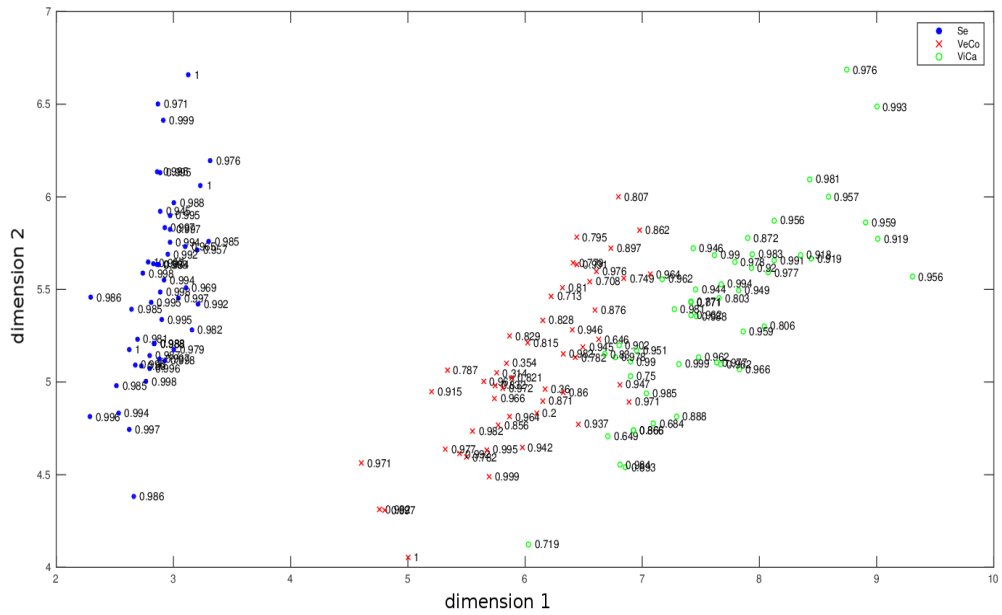


Figure 5.: Projection of the Iris data set using PCA.

502 For KPCA, we plotted the squared cosine values as circles to make the representation  
 503 clearer, especially for the Iris data set as the Iris setosa species are projected next to  
 504 each other. From Figure 6a, we can conclude that in each category, the points that  
 505 have close quality values are located side by side.

506 Furthermore, by comparing the proposed projection method with the one obtained by  
 507 MDS, it can be concluded that, as is the case when using PCA, the points in Figure  
 508 6b are projected by giving more importance to the Iris setosa group. Indeed, almost  
 509 all the red circles (indicating a very good projection) are assigned to the Iris setosa  
 510 species. Moreover, the comparison of the position of points in the reduced space in  
 511 terms of distance between points cannot be viewed in this classical method as the  
 512 points in the reduced space is not in the same metric of the initial distances, whereas  
 513 in our method we have conserved the metric of the initial distances.



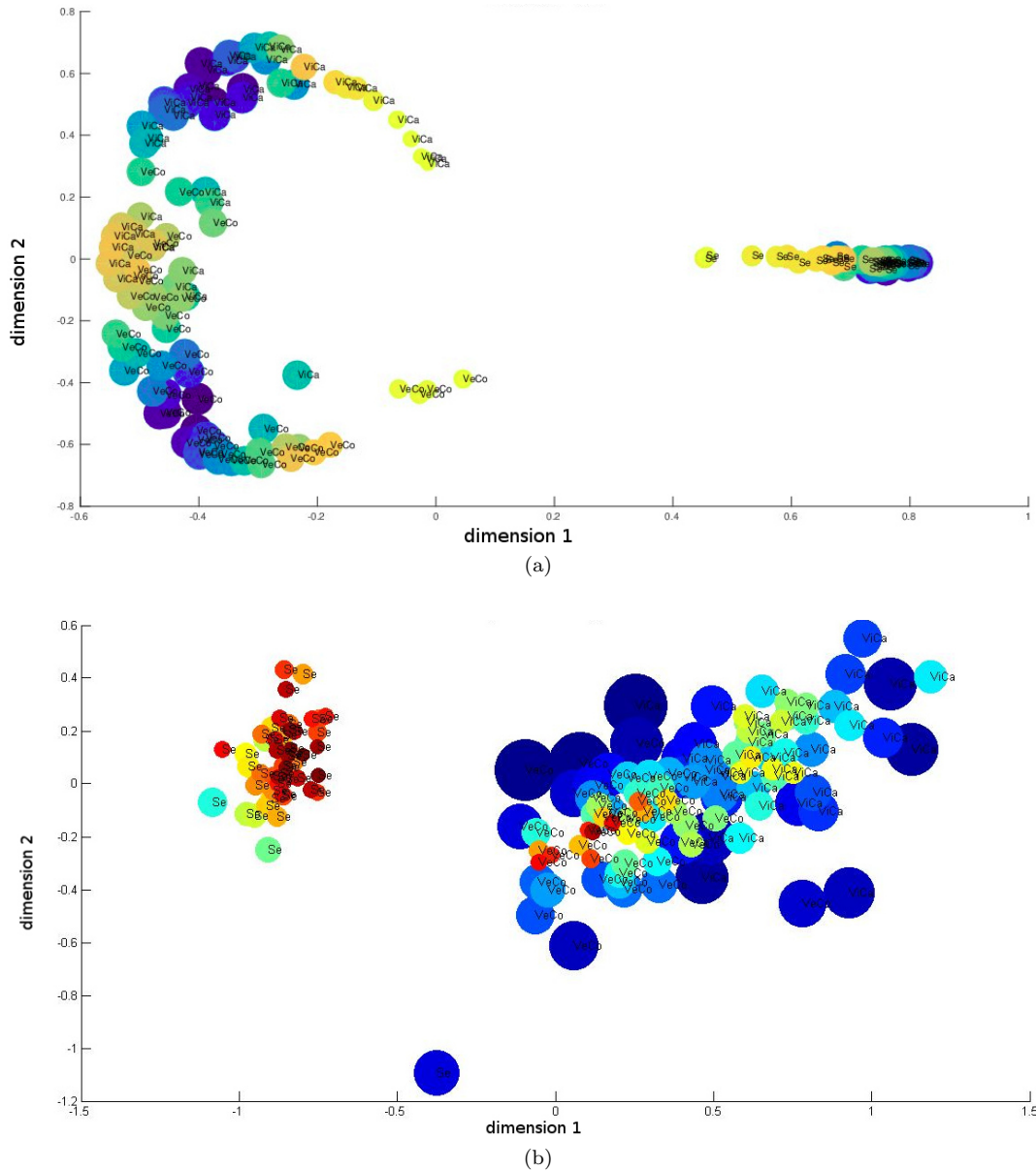


Figure 6.: Projection of the Iris data set using KPCA (a) and MDS (b). The color convention is as follows: the darker the red color of a particular disk, the better the projection. Inversely, the darker the blue color of a particular disk, the worse the projection.

514 **Cars data set:** The projection of points using projection under pairwise distance  
 515 control for the car data set is shown in Figure 7. The expensive cars, the "Audi 100",  
 516 "Alfetta-1.66", "Datsun-200L" and "Renault 30" are well-separated from the low-  
 517 standard cars, the "Lada-1300", "Toyota Corolla", "Citroen GS Club" and "Simca  
 518 1300". Moreover, we can assert that the projected points obtained using projection

519 under pairwise distance control method are well separated as there are no circle inter-  
 520 sections.

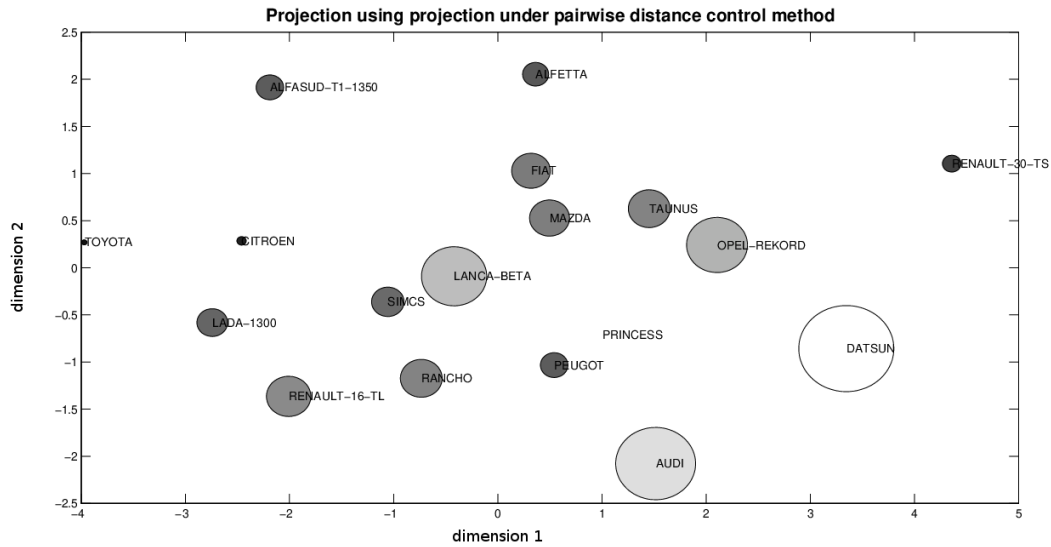


Figure 7.: Projection of the car data set using projection under pairwise distance control.

521 By comparing our projection with the projection obtained using PCA presented in  
 522 Figure 8, it can be shown that in the projection of PCA, there is a group with small  
 523 values of quality measure located at the center, which corresponds to the cars: Lanca-  
 524 Beta, Mazda, Fiat, Simcs and Rancho, and a group with high values of quality measure  
 525 located far from the center. Thus, as shown for the Iris data set, projection under  
 526 pairwise distance control method projects the points without giving any importance  
 527 to the position of the points in the reduced space.

528 Regarding KPCA, we can see in Figure 9a that the points with navy circles are almost  
 529 all located almost around the same y-axis coordinates and the same applies for the  
 530 red circles. So the local quality for KPCA is dependent on the position of the points.  
 531 It can also be noticed that the cars Princess, Mazda, Fiat and Peugeot located in  
 532 the same area with small circles. Therefore, the only conclusion that we arrive at  
 533 is in relation to the size of the circles and to the quality of the projected points.  
 534 However, it is not possible to conclude anything about the closeness of these 4 points  
 535 as the distances here are in the feature space and are not related to the original space.  
 536 In Figure 7, we can however conclude that the two cars, the Mazda and Fiat, are

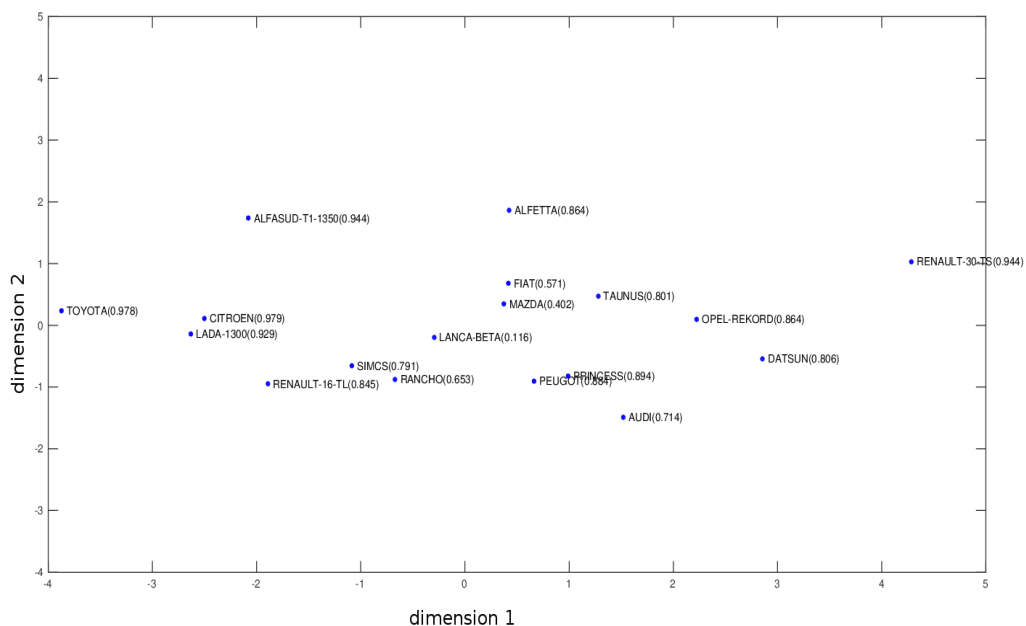


Figure 8.: Projection of the cars data set using PCA.

537 well projected in the reduced space, and they have similar characteristics as these  
538 two cars are close. The same conclusion can be made for the Peugeot and Princess  
539 cars. From this, it is possible to conclude that there is a large difference between the  
540 two cars, the "Toyota" and "Renault 3" as the distance between these two cars is  
541 significant. Conversely, the distance between the "Lada1300" and "Citroen" is small,  
542 thus indicating the closeness of these two cars. Note that these two cars are very well  
543 projected, resulting in a very good interpretation of the distance between them.

544 Therefore, the pairwise distances are meaningful in our method and give an interpre-  
545 tation about the distances between points whereas the distances between the projected  
546 points using PCA, KPCA and MDS are not interpretable as the cosine values and the  
547 Stress-per-point cannot be interpreted as distances. This is a particular strength of our  
548 method. Projection under pairwise distance control suggests an absolute interpretation  
549 whereas the other methods provide a relative one.

550 For the qualitative and functional data sets and using MDS, recall the definition of  
551 the Gram matrix called  $B$  which is equal to  $X'X$  where  $X$  is the coordinate matrix in

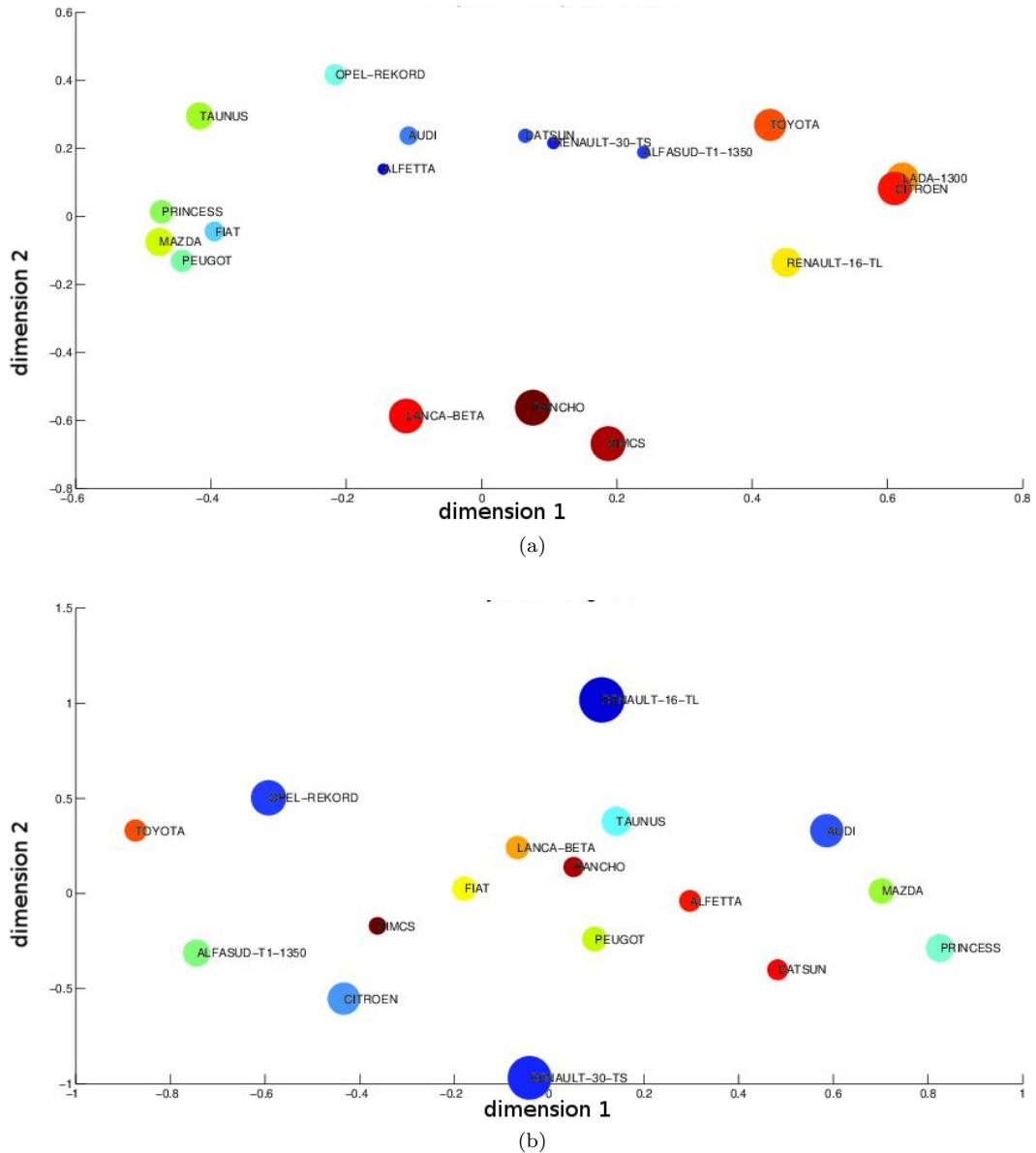


Figure 9.: Projection of the car data set using KPCA (a) and MDS (b).

552 the reduced space. Thus, it is necessary to verify that the matrix  $B$  obtained by the  
 553 MDS method is semi-definite positive to use the squared cosine as the quality measure  
 554 because the starting point of optimization is obtained from MDS. After this, in case  
 555 of positiveness of matrix  $B$ , the quality measure can be calculated.

556 **Soybean data set:** In the projection of the soybean data set, four classes are shown  
 557 in Figure 10 and each class contains the disease number of the class. The whole set of  
 558 points can however be divided in two large classes. Indeed, it is clear that Class 2 is

559 well separated from the other classes as there is no intersection between the circles of  
 560 Class 2 and the circles of other classes. Moreover, Class 1 can be considered as well  
 separated class from Classes 3 and 4 if the largest circle  $D_3$  is not taken into account.

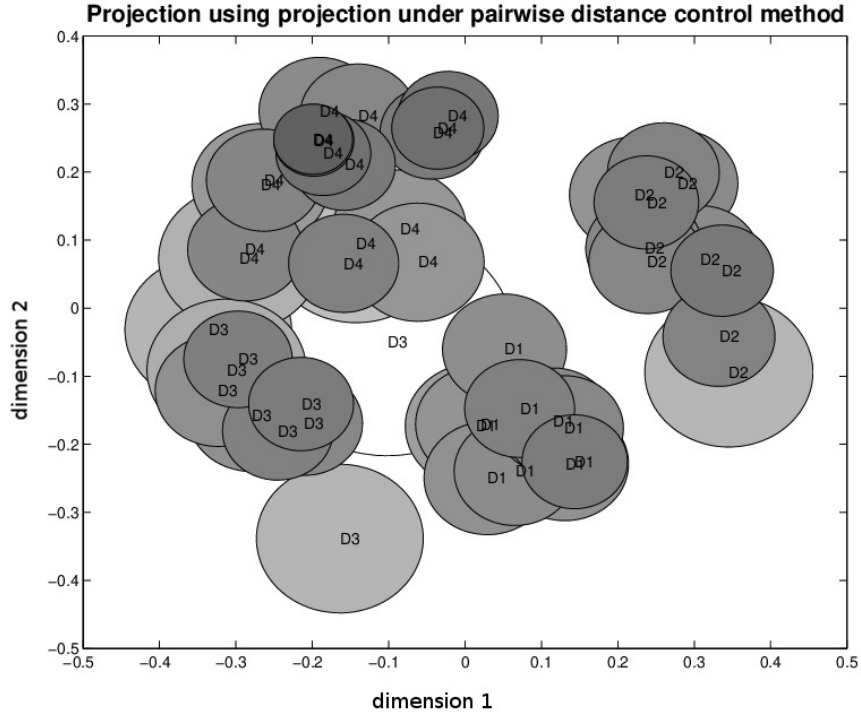


Figure 10.: Projection under pairwise distance control for the soybean data set. Four groups are presented, indexed by D1, D2, D3 and D4.

561

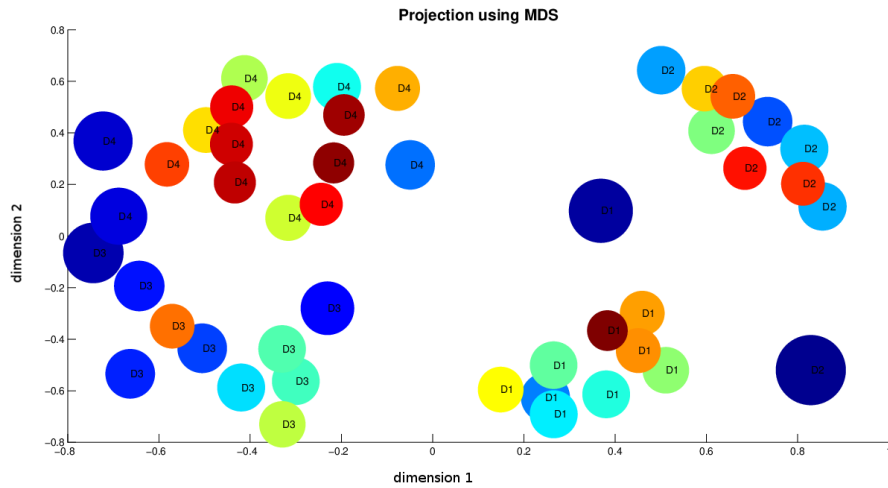


Figure 11.: MDS for the soybean data set. Four groups are presented, indexed by D1, D2, D3 and D4.

562 Classes 3 and 4 are not well separated at all, as there are different intersections between  
 563 the circles of these two classes. This result is shown in Stepp (1984) which labels the  
 564 first two classes as "normal" and the latter two classes as "irrelevant". A comparison  
 565 of results from projection under pairwise distance control with PCA and KPCA is not  
 566 possible for this data set because the matrix  $B$  is not semi-definite positive. Regarding  
 567 Figure 11, it is clear that Class 4 exhibits the worst projection quality, whereas Classes  
 568 1 and 2 show better projection quality. Therefore, it is possible to draw the same  
 569 conclusion for the Iris and car data sets when using MDS as a projection method, the  
 570 projection quality of points is dependent on the class of the points.

571 **Coffee data set:** The coffee data set has been studied in several articles (Briandet  
 572 *et al.* (1996), Bagnall *et al.* (2012)) and different classification methods have shown  
 573 the different groups contained in this data set. The grouping structure obtained can  
 574 be clearly seen in Figures 12 and 13

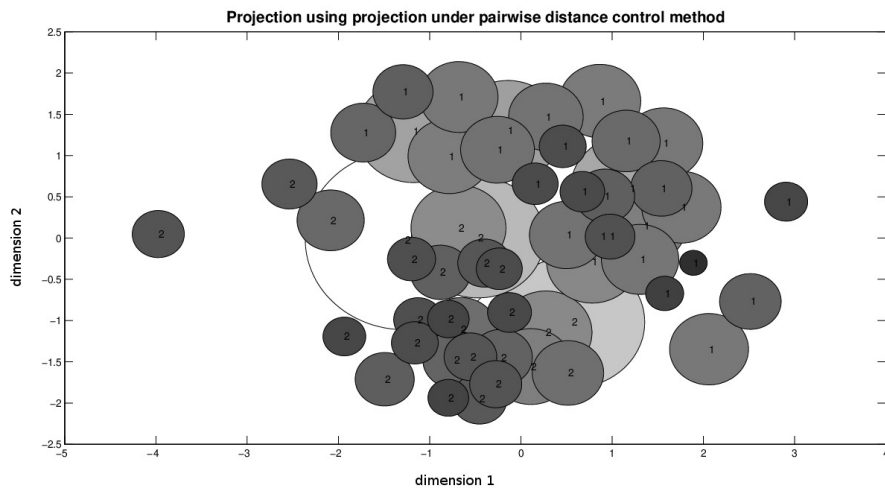
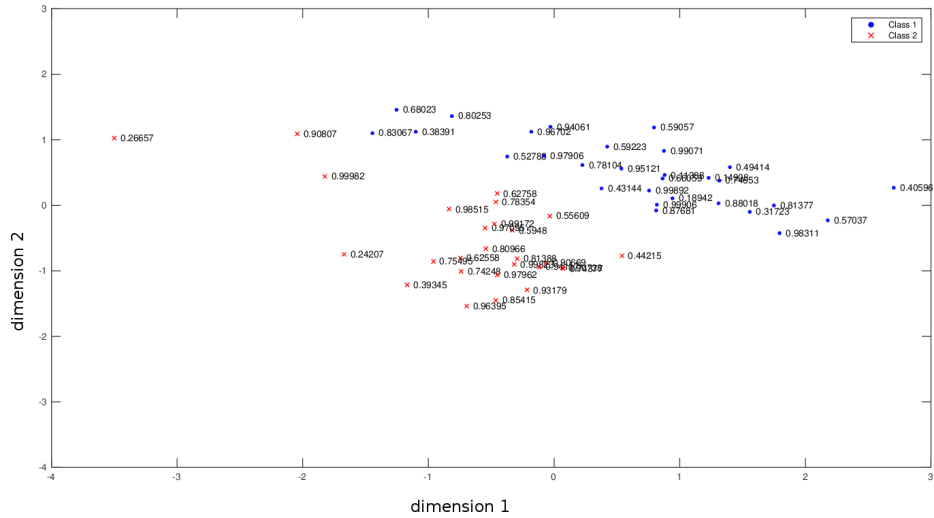


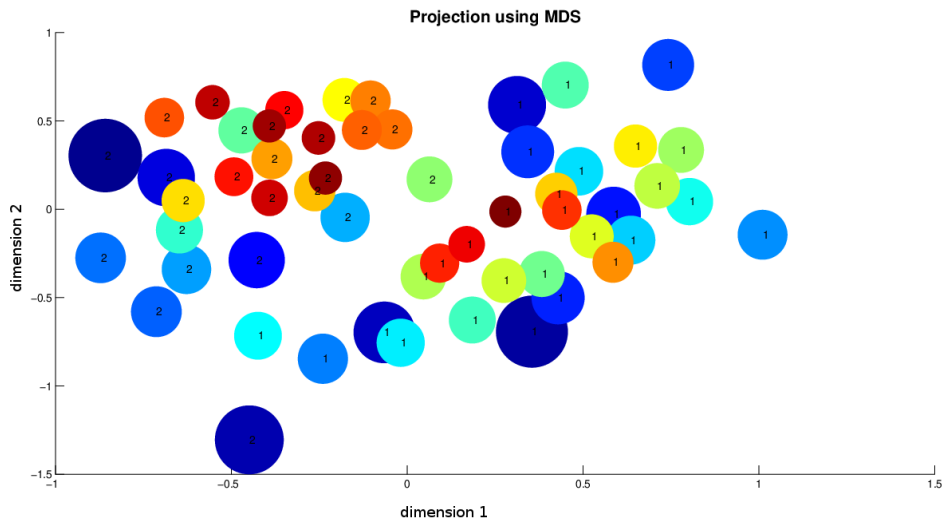
Figure 12.: Projection of the coffee data set using projection under pairwise distance control. Two clusters, indexed 1 and 2, indicate the Arabica and Robusta classes respectively.

575 In Figure 12, we show that we have succeeded in differentiating the Arabica from  
 576 Robusta coffee. These two classes are clearly presented, the first class indexed by  
 577 number 1, corresponding to Arabica coffee, and the second one indexed by number 2,  
 578 corresponding to Robusta coffee. These classes are not well separated in comparison  
 579 with the results of quantitative data, since there are many intersections. Therefore,

580 the representation of the points as circles and not as simple points provides more  
 581 information about the real point classes and shows the points that are at risk of being  
 582 misplaced in a particular class.



(a)



(b)

Figure 13.: Projection of coffee data set using PCA and MDS.

583 Figures 13a and 13b show the projection quality using PCA and MDS respectively.  
 584 As all the eigenvalues of matrix  $B$  are positive, we can compute the quality measure  
 585 given by PCA. Comparing the projection quality of PCA and projection under pairwise  
 586 distance control provided by Figures 13a and 12, respectively, it can be seen that the

587 quality of projection of the set of points is quite steady.

588 Additionally, Algorithm 2 was applied to these data sets. The trace plots of the  
 589 optimization problem  $\mathcal{P}_{r,x}$  are shown in Figure 14 after 5000 iterations. It is important  
 590 to note that the value of the sum of radii  $\sum_{i=1}^n r_i$  decreases rapidly in the first iterations  
 591 and stays roughly constant after 1000 iterations for the different data sets, with the  
 592 exception of the car data sets. Thus, we can decrease the number of iterations from  
 593 5000 to almost 2000, or even 1000, in order to reduce the speed time.

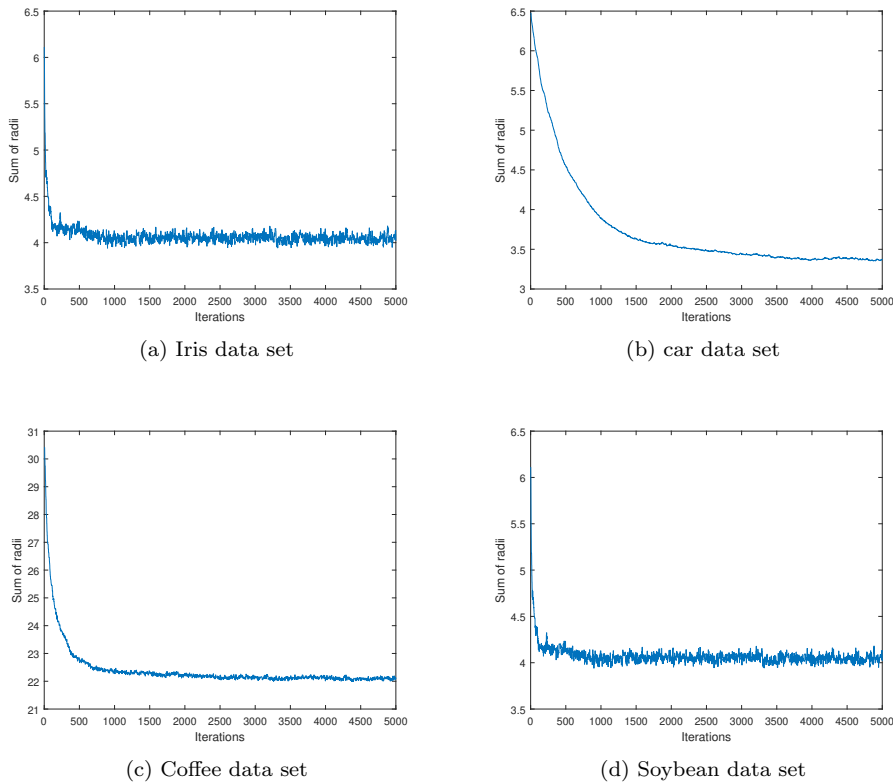


Figure 14.: Trace plots of Metropolis Hastings for different data sets. The x-axis corresponds to the iteration number and the y-axis to the value of  $\sum_{i=1}^n r_i$ .

594 Finally, the computer speed time of the proposed method is compared with that  
 595 using the classical methods. Table 2 shows the computer speed time for the four data  
 596 sets using PCA, KPCA, MDS, Algorithm 1 and Algorithm 2. It is clear that our  
 597 method takes more time than the existing methods. However, Algorithms 1 and 2 are  
 598 expected to significantly increased by using the C++ programming language (instead  
 599 of MATLAB currently) to produce more efficient code. In addition, by comparing the



600 computer speed time of the two algorithms and by referring to Table 1, the solu-  
 601 tions obtained using Algorithm 1 and Algorithm 2 are very close, which indicates that  
 602 Algorithm 2 can be used instead of Algorithm 1 to obtain a better solution faster (be-  
 603 tween two and four times faster). Thus, Algorithm 2 (Metropolis Hastings algorithm)  
 is recommended for use as it takes less time.

Table 2.: Computer speed time (in seconds) using different methods for the four data sets

Computer speed time (sec.)					
	PCA	KPCA	MDS	Algo 1	Algo 2
Iris	3.61	5.21	5.54	1124	600
Cars	2.70	4.17	4.62	671	300
Soybean	–	–	2.65	2036	698
Coffee	3.68	–	3.18	1968	589

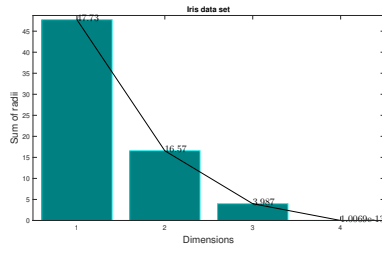
604

#### 605 4.4.2. Dimensionality reduction results

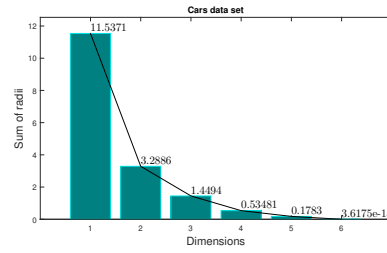
606 Our method can also be directly used to reduce the dimensionality of data (possibly  
 607 using it beyond visualization in  $\mathbb{R}^2$ ). This only requires solving problem  $\mathcal{P}_{r,x}$  using  
 608 different dimension values. In Figure 15, the values of  $\sum_{i=1}^n r_i$  were plotted as a guide  
 609 for choosing the reduced number of variables. This figure shows the values of  $\sum_{i=1}^n r_i$   
 610 for the different data sets using different dimensions. It is clear that the value of  
 611  $\sum_{i=1}^n r_i$  decreases when the dimension increases.

612 The main problem, which is widely posed in dimensionality reduction methods, is  
 613 the determination of the number of components that need to be kept. Many methods  
 614 have been discussed in the literature (Besse (1992); Jolliffe (1986)) to determine  
 615 the dimension of the reduced space, relying on different strategies related to a good  
 616 explanation or a good prediction. Thus, with our method the choice of the reduced  
 617 space dimension is related to the local projection quality of points and how much the  
 618 user is interested in the projection quality of points.

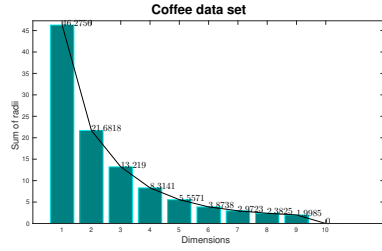
619 Regarding the quantitative data sets (Iris and car), if the main objective of the  
 620 user is to obtain a very good projection quality, then a choice of three components  
 621 against four, for Iris data set and six for the car data set can be a good choice, as the



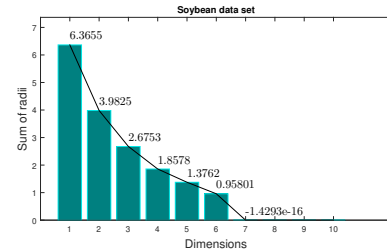
(a) Iris data set



(b) cars data set



(c) Coffee data set



(d) Soybean data set

Figure 15.: Scree plots of  $\sum_{i=1}^n r_i$  for different dimensions for the four data sets.

622 value of  $\sum_{i=1}^n r_i$  is small and there is not a large difference between this value and  
 623 the values for higher dimensions. For the coffee data set, a dimensionality reduction  
 624 from 56 sample time series down to 6 simple extracted features is considered as a good  
 625 choice. As for the soybean data set, a reduced space dimension equal to 4 dimensions  
 626 can be considered as an appropriate reduced space.

627 A comparison of our results with the existing results shows a coherence between  
 628 them. For the Iris data set, Chiu (1996) and Liu and Setiono (1995) concluded  
 629 that the number of variables could be reduced to 2 as the petal length and petal  
 630 width variables are the most important variables from all the variables. For the car  
 631 data set, Saporta (2006) (Table 7.4.1 page 178) noticed that the conservation of two  
 632 dimensions led to the explanation of 88% of inertia, where the inertia term reflects  
 633 the importance of a component. Therefore, these results seem very similar to our  
 634 results, with the important decrease located between dimensions 1 and 2. The other  
 635 reductions are negligible for these two data sets. A selection of variables was studied on  
 636 time series coffee data set by Andrews and McNicholas (2014). Using several analysis  
 637 methods, the number of selected variables ranged between 2 and 13. This result is also  
 638 seen using our method, a number of reduced variables taken between 2 and 9 gives a

639 good projection. Regarding the soybean data set, Dela Cruz shows in his paper Dela  
640 Cruz (2015) that the 35 attributes can be reduced to 15. With our method, we have  
641 succeeded in reducing the attributes to 6 by having a very good projection of points.  
642 Hence, the results presented confirm that the dimension nonlinearly can be reduced  
643 while assessing a reasonable number of dimensions at the same time.

## 644 **5. Conclusion**

645 The purpose of this paper was to outline a new nonlinear projection method based  
646 on a new local measure of projection quality. Of course, in some projection methods,  
647 a local measure is given but this measure cannot be applied unless in cases of linear  
648 projections, and even then it is not suitable for graphical representation.

649 The quality of projection is given here by additional variables called radii, which enable  
650 bound on the original distances to be obtained. We have also shown that the idea can  
651 be written as an optimization problem in order to minimize the sum of the radii  
652 under some constraints. As the solution of this problem cannot be obtained exactly,  
653 we developed a stochastic optimization method.

654 This method has several advantages. Firstly, it is a nonlinear projection method that  
655 takes into account the projection quality of each point individually. Secondly, the  
656 distances between projected points are related to the initial distances between points  
657 offering a way to easily interpret the distances observed in the projection plane. The  
658 projection quality of each point can even then be used outside our method, as a post-  
659 processing of PCA or MDS for example. Finally, it appears to be efficient in terms of  
660 dimensionality reduction for the selection of the dimension of the reduced space based  
661 on the local quality of projection.

662 As perspectives, a lower bound for the optimization problem is needed and this radii  
663 approach could also be applied to other methods.

## 664 **References**

665 Anderson, E. (1935). The Irises of the Gaspé Peninsula. *Bulletin of the American Iris Society*  
666 59:2-5.

667 Andrews, J. L. and McNicholas, P. D. (2014). Variable Selection for Clustering and Classifi-  
668 cation. *Journal of Classification* 31:136-153.

669 Bagnall, A., Davis, L., Hills, J., and Lines, J. (2012). Transformation Based Ensembles for  
670 Time Series Classification. *Proceedings of the 12th SIAM International Conference on Data*  
671 *Mining* 307–319.

672 Berge, C., Froloff, N., Kalathur, R.K., Maumy, M., Poch, O., Raffelsberger, W. and Wicker, N.  
673 (2010). Multidimensional fitting for multivariate data analysis. *Journal of Computational*  
674 *Biology* 17:723–732.

675 Besse, P(1992). PCA stability and choice of dimensionality. *Statistics & Probability Letters*  
676 13:405-410.

677 Boggs, P. T. and Tolle, J. W. (1995). Sequential quadratic programming. *Acta Numer* 4:1–51.

678 Borg, I. and Groenen, P. (2005). *Modern Multidimensional Scaling: Theory and Applications*  
679 (2nd ed.) New York: Springer-Verlag.

680 Boriah, S., Chandola, V., and Kumar, V. (2008). Similarity Measures for Categorical Data:  
681 A Comparative Evaluation. *Proceedings of the SIAM International Conference on Data*  
682 *Mining*.

683 Briandet, R., Kemsley, E. K., and Wilson, R. H. (1996). Discrimination of arabica and robusta  
684 in instant coffee by fourier transform infrared spectroscopy and chemometrics. *Journal of*  
685 *Agricultural and Food Chemistry* 44(1):170–174.

686 Chan, W. W-Y. (2006). A survey on multivariate data visualization in Science and technology.  
687 *Department of Computer Science and Engineering Hong Kong, University of Science and*  
688 *Technology* 8(6):1–29.

689 Chen, Y., Keogh, E., Hu, B., Begum, N., Bagnall, A., Mueen, A. and Batista, G. (2015). *The*  
690 *UCR Time Series Classification Archive*. [www.cs.ucr.edu/~eamonn/time\\_series\\_data/](http://www.cs.ucr.edu/~eamonn/time_series_data/).

691 Cheung, L. W. (2012). Classification approaches for microarray gene expression data analysis.  
692 *Methods in Molecular Biology* 802:73–85.

693 Chinchilli, V. M. and Sen, P. K. (1987). Multivariate Data Analysis: Its Methods. *Chemomet-*  
694 *rics and Intelligent Laboratory Systems* 2:29–36.

695 Cleveland, W. S. and McGill, M. E. (1988). Dynamic Graphics for Statistics. *Wadsworth and*  
696 *Brooks/Cole*, Pacific Grove, Canada.

697 Chiu, S. L. (1996). Method and Software for Extracting Fuzzy Classification Rules by Sub-  
698 tractive Clustering. *Proceedings of North American Fuzzy Information Processing Society*  
699 *Conference*.

700 Cristofari, A., De Santis, M., Lucidi, S. and Rinaldi, F. (2007). A Two-Stage Active-Set Algo-  
701 rithm for Bound-Constrained Optimization. *J. Optim. Theory Appl.* 172(2):369–401.

702 Conn, De A. R., Gould, N. I. M. and Toint, Ph. L. (2000). Trust Region Methods, SIAM.

703 Dela Cruz, G. B. (2015). Comparative Study of Data Mining Classification Techniques over  
704 Soybean Disease by Implementing PCA-GA. *International Journal of Engineering Research*  
705 *and General Science* 3(5):6–11.

706 Dempster, A. P. (1971). An overview of multivariate data analysis. *Journal of Multivariate*  
707 *Analysis* 1(3):316–346.

708 Golub, T. R., Slonim, D. K., Tamayo, P., Huard, C., Gaasenbeek, M., Mesirov, J. P., Coller,  
709 H., Loh, M. L., Downing, J. R., Caligiuri, M. A., Bloomfield, C. D. and Lander, E. S. (1999).  
710 Molecular classification of cancer: class discovery and class prediction by gene expression  
711 monitoring. *Science* 286:531–537.

712 Ieva, F., Paganoni, A.M., Pigoli, D., and Vitelli., V. (2012). Multivariate functional clustering  
713 for the analysis of ECG curves morphology, *Journal of the Royal Statistical Society. Applied*  
714 *Statistics, series C* 62(3):401–418.

715 Inselberg, A. (1985). The Plane with Parallel Coordinates. *Special Issue on Computational*  
716 *Geometry, The Visual Computer* 1:69–91.

717 Jackson, J. (1991). A Users Guide to Principal Components, *John Wiley & Sons, New York*.

718 Jagannathan, R. and Ma, T. (2003). Risk reduction in large portfolios: why imposing the  
719 wrong constraints helps. *The Journal of Finance* 58:1651–1683.

720 Johansen, A. M. and Evers, L. (2007). *Monte Carlo Methods*. Department of Mathematics,  
721 University of Bristol.

722 Jolliffe, I. T. (1986). *Principal Component Analysis*, Springer, New York

723 Keim, D. A. and Kriegel, H. P. (1996). Visualization Techniques for Mining Large Databases:  
724 A Comparison. *IEEE Transactions on Knowledge and Data Engineering* 8(6):923-938.

725 Lee, J. A. and Verleysen, M. (2007). *Nonlinear Dimensionality Reduction*. Springer.

726 Liu, H. and Setiono, R. (1995). Chi2: feature selection and discretization of numeric attributes.  
727 *Proceedings Seventh International Conference on Tools with Artificial Intelligence*.

728 Febrero-Bande, M., Oviedo de la Fuente, M. (2011). Statistical Computing in Functional Data  
729 Analysis: The R Package fda.usc. *Journal of statistical software* 51(4).

730 Mardia, K. V., Kent, J. T. and Bibby, J. M. (1979). *Multivariate analysis*, Academic Press,  
731 London.

732 Murty, K. G. (1983). *Linear programming*. John Wiley & Sons, New York.

- 733 Roweis, S. and Saul, L. (2000). Nonlinear dimensionality reduction by locally linear embedding,  
734 *Science* 290(5500):2323–2326..
- 735 Sammon, J. (1969). A nonlinear mapping for data structure analysis. *IEEE Transactions on*  
736 *Computers* 18(5):401–409.
- 737 Saporta, G. (2006). Probabilités, analyse des données et statistique. *Technip*.
- 738 Schölkopf, B. (1998). Nonlinear Component Analysis as a Kernel Eigenvalue Problem. *Neural*  
739 *Computation* 10(5): 1299–1319.
- 740 Stepp, R. (1984). Conjunctive conceptual clustering. Doctoral dissertation, department of com-  
741 puter science, university of Illinois, Urbana-Champaign, IL.
- 742 Svante, W., C. Albano, W. J. DunnIII, U. Edlund, K. Esbensen, P. Geladi, S. Hellberg, E.  
743 Johansson, W. Lindberg , M. Sjostrom. (1984). Multivariate Data Analysis in Chemistry.  
744 *Chemometrics* 138:17–95.
- 745 Tenenbaum, J. B., De Silva, V. and Langford, J. C. (2000). A global geometric framework for  
746 nonlinear dimensionality reduction. *science*, 290(5500):2319-2323.
- 747 Togerson, W. S. (1958). Theory and methods of scaling, New York: Wiley.
- 748 Van der Hilst, R., de Hoop, M., Wang, P., Shim, S.-H., Ma, P. and Tenorio, L. (2007).  
749 Seismo-stratigraphy and thermal structure of earth’s core-mantle boundary region. *Science*  
750 315:1813–1817.
- 751 Wong, E. (2011). Active-Set Methods for Quadratic Programming. Ph.D. thesis, university of  
752 California, San Diego.

# Appendix

## 754 Proof of proposition 3.1

Let us consider a point  $x_i$  such that for an index  $j$ , the following inequality is saturated:

$$|d_{ij} - \|x_i - x_j\|| \leq r_i + r_j,$$

755 and the other inequalities involving  $i$  are not saturated. Then, the corresponding solu-  
 756 tion can be improved by moving  $x_i$  along the line  $x_j - x_i$  in order to decrease  $r_i$  and  
 757  $|d_{ij} - \|x_i - x_j\||$ .

758 **Proof.** The above condition means that  $x_i$  is rewritten as  $x_i + a(x_j - x_i)$  with  $a \in \mathbb{R}$   
 759 and we look for  $a$  such that  $|d_{ij} - \|x_i + a(x_j - x_i) - x_j\|| < r_i + r_j$ . In particular  $a \leq 0$   
 760 if  $d_{ij} - \|x_i - x_j\| \geq 0$  and is otherwise  $> 0$ . Let us now consider the other inequalities  
 761 corresponding to index pairs  $(i, k)$  with  $k \neq j$ . For each of them,  $\exists a \in [a'_k, a''_k]$  with  
 762  $a'_k < 0$  and  $a''_k > 0$  such that

$$|d_{ij} - \|x_i + a(x_j - x_i) - x_j\|| \leq r_i + r_j,$$

763 as these constraints are unsaturated. Finally, taking  $a$  different from 0 in  $[a', a'']$  with  
 764  $a' = \max_k a'_k$  and  $a'' = \min_k a''_k$ , all constraints involving  $i$  get unsaturated so that  $r_i$   
 765 can be decreased, thereby decreasing the objective function. Depending on whether  $a$   
 766 must be negative or positive, we take  $a = a'$  or  $a = a''$  respectively.

768 **Proof of proposition 3.2**

769 Let  $r_1, \dots, r_n; x_1, \dots, x_n$  be a feasible solution of  $\mathcal{P}_{r,x}$ , if  $\exists a$  such that  $\eta(a) < \sum_{i=1}^n r_i$

770 with  $\eta(a) = \sum_{1 \leq i < j \leq n} |d_{ij} - a\|x_i - x_j\||$ , then  $\exists \tilde{r}_1, \dots, \tilde{r}_n$  a solution of  $\mathcal{P}_{r,a}$  such that

771 
$$\sum_{i=1}^n \tilde{r}_i < \sum_{i=1}^n r_i.$$

772 **Proof.** Let us consider  $r_1, \dots, r_n; x_1, \dots, x_n$  a feasible solution of problem  $\mathcal{P}_{r,x}$  and

773  $a, \tilde{r}_1, \tilde{r}_2, \dots, \tilde{r}_n$  a solution of  $\mathcal{P}_{r,a}$  where  $a$  is kept constant. For the solution of  $\mathcal{P}_{r,a}$ , for

774 each point  $i$ , we have a certain saturated constraint associated to point  $k$  denoted by

775  $C_{ik(i)}$ , otherwise we can easily saturate it using proposition 3.1. Thus, we have:

$$\begin{aligned} |d_{i1} - a\|x_i - x_1\|| &\leq \tilde{r}_i + \tilde{r}_1 \\ &\vdots \\ |d_{ik(i)} - a\|x_i - x_{k(i)}\|| &= \tilde{r}_i + \tilde{r}_{k(i)} \\ &\vdots \\ |d_{ij} - a\|x_i - x_j\|| &\leq \tilde{r}_i + \tilde{r}_j \\ &\vdots \\ |d_{in} - a\|x_i - x_n\|| &\leq \tilde{r}_i + \tilde{r}_n. \end{aligned}$$

776 Then,  $|d_{ik(i)} - a\|x_i - x_{k(i)}\|| = \tilde{r}_i + \tilde{r}_{k(i)} \geq \tilde{r}_i$ . By summing for all points  $i$ , for  $i =$

777  $1, \dots, n$ , we obtain:

$$\sum_{i=1}^n |d_{ik(i)} - a\|x_i - x_{k(i)}\|| \geq \sum_{i=1}^n \tilde{r}_i.$$

778 Thus,  $\sum_{1 \leq i < j \leq n} |d_{ij} - a\|x_i - x_j\|| \geq \sum_{i=1}^n |d_{ik(i)} - a\|x_i - x_{k(i)}\|| \geq \sum_{i=1}^n \tilde{r}_i.$

779 Note  $\eta(a) = \sum_{1 \leq i < j \leq n} |d_{ij} - a\|x_i - x_j\||$ , then if  $\eta(a) < \sum_{i=1}^n r_i$  there is a solution of  $\mathcal{P}_{r,a}$

780 such that  $\sum_{i=1}^n \tilde{r}_i < \sum_{i=1}^n r_i.$  □